

Revisiting Very High Energy Gamma-Ray Absorption in Cosmic Propagation under the Combined Effects of Axion-Like Particles and Lorentz Invariance Violation

Longhua Qin¹, Jiancheng Wang^{2,3}, Chuyuan Yang^{2,3,*}, Huaizhen Li^{1,*}, Quanguai Gao^{1,*}, Ju Ma¹, Ao Wang¹, Weiwei Na¹, Ming Zhou^{2,3}, Zunli Yuan⁴, Chunxia Gu⁵ and Guangbo Long⁶

1. *Department of Physics, Yuxi Normal University, Yuxi, Yunnan, 653100, People's Republic of China*
2. *Yunnan Observatory, Chinese Academy of Sciences, Kunming, Yunnan, 650011, People's Republic of China*
3. *Key Laboratory for the Structure and Evolution of Celestial Objects, Chinese Academy of Sciences, Kunming, Yunnan, 650011, People's Republic of China*
4. *Department of Physics and Synergistic Innovation Center for Quantum Effects and Applications, Hunan Normal University, Changsha, Hunan, 410081, People's Republic of China*
5. *Oxbridge College, Kunming University of Science and Technology, Kunming, Yunnan, 650011, People's Republic of China*
6. *School of Intelligent Engineering, Shaoguan University, Shaoguan, Guangdong, 512005, People's Republic of China*

* *Corresponding author: lhz@yxnu.edu.cn; qggao@yxnu.edu.cn; chyy@ynao.ac.cn*

ABSTRACT

Very-high-energy (VHE; $E \gtrsim 100$ GeV) gamma rays are expected to experience strong attenuation during cosmological propagation due to electron-positron pair production on the extragalactic background light (EBL). Recent observations of GRB 221009A ($z = 0.151$), including photons up to ~ 18 detected by LHAASO and a ~ 300 TeV event reported by Carpet-3, suggest a higher-than-expected transparency of the Universe at extreme energies. These observations cannot be explained by standard EBL absorption alone; moreover, neither Lorentz invariance violation (LIV) nor photon-axion-like particle (ALP) oscillations, when considered in isolation, appear sufficient to account for the survival of such photons over cosmological distances. In this work, we propose a joint propagation

scenario that incorporates photon-ALP mixing in astrophysical magnetic fields together with subluminal quadratic LIV corrections to the $\gamma\gamma$ pair-production threshold. Applying this framework to the broadband gamma-ray spectrum of GRB 221009A, we show that ALPs with coupling ($g_{a\gamma} = 1.685 \times 10^{-10} \text{GeV}^{-1}$) and mass ($m_a = 9.545 \times 10^{-8} \text{eV}$), combined with a quadratic LIV energy scale ($E_{\text{LIV},2} = 1.30 \times 10^{-7} E_{\text{Pl}}$) adopted from the literature, can significantly enhance the photon survival probability in the energy range (10-300) TeV. The resulting enhancement exceeds that obtained from either ALP mixing or LIV effects alone. These results indicate that a combined ALP-LIV scenario may provide a viable interpretation of the extreme-energy gamma-ray observations of GRB 221009A and highlight the potential of VHE gamma-ray measurements as probes of physics beyond the Standard Model.

Subject headings: Gamma-ray bursts; Cosmic background radiation; Dark matter; Quantum gravity

1. Introduction

Very-high-energy (VHE) gamma rays, typically defined as photons with energies exceeding 100 GeV, are expected to undergo substantial attenuation as they propagate through the intergalactic medium. This attenuation is primarily caused by interactions with the extragalactic background light (EBL), which lead to electron-positron pair production ($\gamma\gamma \rightarrow e^+e^-$). Beyond this primary absorption process, the resulting e^+e^- pairs can further up-scatter cosmic microwave background (CMB) photons via inverse-Compton interactions, thereby initiating electromagnetic cascades that regenerate secondary gamma rays at lower energies. Together, these processes can significantly reshape the observed spectra of high-energy gamma-ray sources. Moreover, due to the strong EBL absorption, gamma rays with energies above ~ 30 TeV are expected to have extremely limited propagation distances on cosmological scales, making their detection particularly challenging (see e.g., Qin et al. 2023; Domínguez et al. 2013).

Despite theoretical expectations of substantial attenuation due to pair production with EBL, observations of VHE gamma rays from distant blazars consistently reveal a level of transparency exceeding standard model predictions (see e.g., Carmona et al. 2024). This tension poses a significant challenge to our understanding of gamma-ray propagation. Initial evidence arose from H.E.S.S. observations of blazars such as H 2356-309 ($z = 0.165$) and 1ES 1101-232 ($z = 0.186$), whose spectra could only be reconciled with EBL densities substantially below established models (Aharonian et al. 2006). Additional support came

from MAGIC observations of the high-redshift AGN 3C 279 ($z = 0.54$) (MAGIC Collaboration et al. 2008). A systematic trend of reduced absorption in the VHE spectral slopes of AGN at $z > 0.2$ was also reported by De Angelis et al. (2013), further reinforcing the anomaly. Besides, the recent detection of multi-TeV gamma rays from GRB 221009A, including photons up to 18 TeV observed by LHAASO (Cao et al. 2023) and a 251 TeV photon candidate reported by the Carpet collaboration (Dzhappuev et al. 2022) later updated as 300_{+42}^{-30} TeV by (Dzhappuev et al. 2025), presents a significant tension with standard models of gamma-ray propagation. Under conventional EBL attenuation models, the observed spectrum-associated with the most luminous GRB ever recorded-would necessitate an unphysical intrinsic spectral upturn to account for the transmitted flux at these energies, even when adopting the lowest EBL density estimates. This discrepancy strongly motivates the investigation of beyond-standard-model scenarios, such as axion-like particles (ALPs) and Lorentz invariance violation (LIV), that could effectively reduce EBL-induced attenuation and increase the gamma-ray transparency of the universe.

ALPs and LIV provide distinct frameworks to explain the anomalous transparency of VHE gamma rays. ALPs introduce a new light pseudo-scalar particle that can oscillate with photons in cosmic magnetic fields, allowing gamma rays to partially evade attenuation by EBL. Such ALPs need to convert back to photons in the vicinity of our observatories, e.g., in the galactic magnetic field. In addition, LIV scenarios may introduce a preferred reference frame, allow otherwise forbidden processes (see e.g., photon decays or vacuum Cherenkov radiation; Lehnert & Potting 2004; Saveliev & Alves Batista 2024), and modify fundamental interaction cross-sections (e.g., Carmona et al. 2024). These effects can lead to additional energy losses in high-energy electromagnetic cascades, thereby affecting the propagation of high-energy gamma-ray photons in the intergalactic medium. Historically, several studies have shown that photon-ALPs mixing can enhance the transparency of the Universe to VHE gamma rays (e.g., de Angelis et al. 2008; Long et al. 2020; Cao et al. 2023; Chen et al. 2024), while interest in LIV-induced modifications to the pair-production threshold grew following observations of high energy blazars (e.g., Kifune 1999; Stecker & Glashow 2001) and, more recently, gamma ray bursts such as GRB 221009A (e.g., Finke & Razzaque 2023; Zheng et al. 2023). Searches for ALP-induced spectral irregularities have constrained ALP-photon couplings across wide mass ranges (see e.g., Ajello et al. 2016), and observations of rapid TeV variability in gamma-ray bursts have set stringent limits on LIV energy scales (see e.g., Acciari et al. 2020). However, there is no fundamental reason to exclude the simultaneous presence of ALPs and LIV in explaining the anomalous transparency of gamma rays over cosmological distances (Galanti & Roncadelli 2025). While photon-LP mixing (e.g., de Angelis et al. 2008; Long et al. 2020; Cao et al. 2023; Chen et al. 2024) and subluminal Lorentz invariance violation (LIV)-induced modifications to the pair-

production threshold (e.g., Kifune 1999; Stecker & Glashow 2001; Finke & Razzaque 2023; Zheng et al. 2023) have each been extensively explored as possible explanations for anomalies in VHE gamma-ray transparency-including recent applications to the LHAASO and Carpet-3 observations of GRB 221009A-neither mechanism, when considered in isolation, is able to reproduce the broadband spectrum over the full 10–300 TeV range without invoking extreme parameter choices or encountering tension with independent constraints. These include air-shower limits on LIV energy scales (e.g., Galaverni & Sigl 2008; Ellis et al. 2019) and bounds on ALP couplings inferred from spectral irregularities and other astrophysical probes (e.g., Horns et al. 2012; Acciari et al. 2020). Recent quantitative analyses of the combined LHAASO-Carpet-3 fluence spectrum by Satunin & Troitsky (2025) indicate that ALP-induced effects can provide an improved statistical description compared to LIV-only scenarios, although the two mechanisms are still treated independently.

Based on the above considerations, we construct a model of TeV gamma-ray absorption that simultaneously accounts for both ALPs and LIV, and evaluate its viability using observational data from GRB 221009A. As the most energetic gamma-ray burst ever recorded (redshift $z = 0.151$) (de Ugarte Postigo et al. 2022). GRB 221009A exhibits exceptional brightness and broad spectral coverage (Cao et al. 2019, 2023), offering a unique opportunity to probe $\gamma\gamma$ attenuation over cosmological distances. More than 6×10^4 gamma-ray events with energies between 200 GeV and 7 TeV were detected by the LHAASO Water Cherenkov Detector Array (WCDA) within 3000 s after the Fermi-GBM trigger (Cao et al. 2023). LHAASO also reported the first detection of photons with energies exceeding 10 TeV from a gamma-ray burst, GRB 221009A (Cao et al. 2023). The Kilometer Square Array (KM2A) recorded 142 photon-like events in the 3–20 TeV range during 230–900 s after the trigger, compared to an expected background of 16.7 events, among which nine events have reconstructed energies $\gtrsim 10$ TeV and background probabilities between 0.045 and 0.17. In addition, the Carpet-3 air shower array at the Baksan Neutrino Observatory reported the detection of an air-shower event spatially and temporally coincident with GRB 221009A, with an estimated primary energy of 300_{-38}^{+43} TeV (Dzhappuev et al. 2025).

We first compute the photon survival probability, $P_{\gamma \rightarrow \gamma}(E, z)$, for VHE gamma rays under three scenarios: ALP-only, LIV-only, and the combined ALP-LIV framework. Using the survival probabilities derived in each case, we then perform spectral fits to the multi-band observations of the GRB. For the ALP-LIV case, the fitting is carried out within the simplified hybrid model described above.

This paper is organized as follows. Section 2 outlines the physical processes relevant to the propagation of high-energy gamma rays. Specifically, we discuss: (I) the prompt gamma-ray emission and attenuation due to interactions with the EBL in Section 2.1; (II)

ALP oscillations in external magnetic fields in Section 2.2; (III) the impact of LIV on the $\gamma\gamma \rightarrow e^+e^-$ pair-production process in Section 2.3; and (IV) the combined effects of ALPs and LIV, together with the corresponding model simplifications adopted in this work, in Section 2.4. Finally, Section 4 summarizes our results and presents the discussion and conclusions.

2. Model and strategy

2.1. Prompt gamma-ray spectrum and absorption on EBL

To reconstruct the intrinsic emission spectrum, we adopt a power-law form, $\phi_{\text{PL}}(E) = \phi_0(E/E_0)^{-\alpha}$, where ϕ_0 is the normalization constant and $E_0 = 1$ TeV is the reference energy and α denotes the spectral index. The resulting observed spectral energy distribution (SED) is then given by

$$E^2 \frac{dN}{dE} = P_{\gamma \rightarrow \gamma}(E, z) \phi_{\text{PL}}(E), \quad (1)$$

in units of $\text{erg cm}^{-2} \text{s}^{-1}$.

The optical depth $\tau(E, z)$ for a gamma-ray photon with observed dimensionless energy $\epsilon_s = E/(m_e c^2)$, interacting with background photons of proper-frame energy density $u_p(\epsilon_p; z)$, is given by Gould & Schröder (1967)

$$\begin{aligned} \tau(E, z) = & \frac{c\pi r_e^2}{\epsilon_s^2 m_e c^2} \int_0^z \frac{dz'}{(1+z')^2} \left| \frac{dt_*}{dz'} \right| \\ & \times \int_{\frac{1}{\epsilon_s(1+z')}}^{\infty} d\epsilon_p \frac{\epsilon_p u_p(\epsilon_p; z')}{\epsilon_p^4} \bar{\phi}(\epsilon_p \epsilon_s (1+z')), \end{aligned} \quad (2)$$

where r_e is the classical electron radius, m_e is the electron mass, and $\bar{\phi}(s_0)$ encodes the pair-production cross-section as a function of the center-of-mass energy squared (see e.g., Gould & Schröder 1967). The differential time-redshift relation in a standard flat Λ CDM cosmology is:

$$\frac{dt}{dz} = \frac{-1}{H_0(1+z)\sqrt{\Omega_m(1+z)^3 + \Omega_\Lambda}}, \quad (3)$$

here, a flat Λ CDM cosmology is adopted, where $\Omega_\Lambda = 0.7$, $\Omega_M = 0.3$, and $H_0 = 70 \text{ km s}^{-1} \text{ Mpc}^{-1}$. Additionally, the unprimed and primed quantities denote the quantities in the observer's frame and the co-moving frame, respectively.

2.2. ALP-photon oscillation in external magnetic fields

ALPs are pseudo-scalar bosons predicted in various extensions of the Standard Model, particularly in string theory and extra-dimensional frameworks. Unlike the Quantum Chromodynamics (QCD) axion (see e.g., Peccei & Quinn 1977), ALPs are not required to solve the strong CP problem and can span a wide parameter space in mass m_a and photon coupling $g_{a\gamma}$ (see e.g., Abbott & Sikivie 1983; Conlon 2006). Their interaction with photons is described by the Lagrangian:

$$\mathcal{L}_{\text{int}} = -\frac{1}{4}g_{a\gamma}aF_{\mu\nu}\tilde{F}^{\mu\nu} = g_{a\gamma}a\mathbf{E}\cdot\mathbf{B}, \quad (4)$$

where a is the ALPs field, $F_{\mu\nu}$ the electromagnetic field tensor, and $\tilde{F}^{\mu\nu}$ its dual. This coupling enables photon-ALP conversions in external magnetic fields (Raffelt & Stodolsky 1988), a process that can significantly affect high energy photon propagation over cosmological distances.

The evolution of an photon-ALP beam propagating through an external magnetic field along the z -axis is governed by a Schrödinger-like equation that accounts for mixing between photons and ALPs. The system is described by the state vector $\psi(z) = (A_x, A_y, a)^T$,

$$i\frac{d\psi(z)}{dz} = M\psi(z), \quad (5)$$

where A_x and A_y denote the photon amplitudes for linear x - and y -polarizations, and a is the ALPs amplitude. The mixing matrix M , expressed in the interaction basis (Long et al. 2020), is given by:

$$M = \begin{pmatrix} \Delta_{\perp} & 0 & 0 \\ 0 & \Delta_{\parallel} & \Delta_{a\gamma} \\ 0 & \Delta_{a\gamma} & \Delta_{aa} \end{pmatrix}, \quad (6)$$

where $\Delta_{\perp} = \Delta_{\text{pl}} + 2\Delta_{\text{QED}} + \Delta_{\text{CMB}} + \frac{i}{2\lambda_{\gamma}}$, and $\Delta_{\parallel} = \Delta_{\text{pl}} + \frac{7}{2}\Delta_{\text{QED}} + \Delta_{\text{CMB}} + \frac{i}{2\lambda_{\gamma}}$ represent the effective dispersion relations for the x - and y -polarized photon modes, including contributions from plasma effects, vacuum birefringence due to quantum electrodynamics (QED), photon scattering (Dobrynina et al. 2015) with the cosmic microwave background (CMB), and absorption by EBL (e.g., Long et al. 2020). Noted from Eq. (4) that ALPs couple only to the photon polarization component lying in the plane defined by the transverse magnetic field B_T and the propagation direction. By choosing a coordinate frame in which B_T is aligned along the y -axis, only the A_y component mixes with the ALPs, thereby

simplifying the dynamics. The off-diagonal term $\Delta_{a\gamma} = \frac{1}{2}g_{a\gamma}B_T$ quantifies the photon–ALPs coupling strength, proportional to the photon–ALPs coupling constant $g_{a\gamma}$ and the transverse magnetic field B_T . The ALPs diagonal term $\Delta_{aa} = -\frac{m_a^2}{2E_\gamma}$ accounts for the effective mass contribution of the ALPs, where E_γ is the photon energy. The numerical values for the different Δ can be found in Horns et al. (2012):

$$\Delta_{a\gamma} \simeq 1.52 \times 10^1 \left(\frac{g_{a\gamma}}{10^{-11} \text{ GeV}^{-1}} \right) \left(\frac{B_T}{10^{-9} \text{ G}} \right) \text{ kpc}^{-1}, \quad (7)$$

$$\Delta_a \simeq -7.8 \times 10^{-3} \left(\frac{m_a}{10^{-3} \text{ TeV}} \right)^2 \left(\frac{E}{10 \text{ eV}} \right)^{-1} \text{ kpc}^{-1}, \quad (8)$$

$$\Delta_{\text{pl}} \simeq -1.1 \times 10^{-10} \left(\frac{E}{\text{TeV}} \right)^{-1} \left(\frac{n_e}{10^{-3} \text{ cm}^3} \right) \text{ kpc}^{-1}, \quad (9)$$

where n_e denotes the electron number density. The plasma term Δ_{pl} is primarily relevant in relatively dense astrophysical environments, such as the host galaxy or the Milky Way disk. In the intergalactic medium, its contribution becomes negligible due to the extremely low electron density.

The system’s statistical evolution is captured by the density matrix $\rho(z) = \psi(z)\psi^\dagger(z)$, which obeys the von Neumann-like equation (Bassan et al. 2010):

$$i \frac{d\rho(z)}{dz} = [\rho(z), M], \quad (10)$$

ensuring the conservation of probability and Hermiticity. In a homogeneous region of size Δz , the formal solution is (e.g., Horns et al. 2012; De Angelis et al. 2013):

$$\psi(z + \Delta z) = U\psi(z), \quad \text{with} \quad U = \exp(-iM\Delta z), \quad (11)$$

$$\rho(z + \Delta z) = U\rho(z)U^\dagger, \quad (12)$$

where U is the unitary evolution operator over the interval Δz .

For an initially unpolarized photon beam with no ALPs component, the initial density matrix is:

$$\rho(0) = \frac{1}{2} \begin{pmatrix} 1 & 0 & 0 \\ 0 & 1 & 0 \\ 0 & 0 & 0 \end{pmatrix}. \quad (13)$$

The probability of a photon remaining a photon after propagation is obtained by tracing over the photon subspace (e.g., Horns et al. 2012; De Angelis et al. 2013; Long et al. 2020):

$$P_{\gamma \rightarrow \gamma}(z) = \text{Tr} \left[\begin{pmatrix} 1 & 0 & 0 \\ 0 & 1 & 0 \\ 0 & 0 & 0 \end{pmatrix} \rho(z) \right] = \rho_{11}(z) + \rho_{22}(z), \quad (14)$$

while the photon-to-ALPs conversion probability is $P_{\gamma \rightarrow a}(z) = \rho_{33}(z)$.

2.3. Effects of LIV on pair production process

Lorentz invariance, a cornerstone of special relativity, may be violated in some quantum gravity frameworks such as string theory and loop quantum gravity (see e.g., Amelino-Camelia et al. 1998; Mattingly 2005; Ellis et al. 2008). In such LIV scenarios, the photon dispersion relation is modified as

$$E^2 - p^2 c^2 = \pm E^2 \left(\frac{E}{E_{\text{QG}}} \right)^n, \quad (15)$$

where E_{QG} is the quantum gravity scale (near $E_{\text{Planck}} \sim 10^{28}$ eV), and n denotes the leading-order correction, that $n = 1$ or 2 corresponds to linear or quadratic leading-order LIV corrections, respectively. The “+” represents superluminal LIV and the “−” sign corresponds to the subluminal case. LIV leads to two notable astrophysical consequences. First, photon speed is energy-dependent, resulting in an energy-dependent time delay for photons emitted simultaneously from distant transients such as GRBs. Time-of-flight measurements from such sources have placed lower bounds on E_{QG} (see e.g. Abdo et al. 2009; Ellis et al. 2019). Second, and more relevant to gamma ray absorption, LIV exerts substantial impacts on the propagation of TeV-PeV gamma rays in intergalactic space by modifying interaction kinematics and enabling novel processes forbidden in the Standard Model. For electromagnetic processes relevant to gamma rays, superluminal LIV scenarios permit photon decay in vacuum, and the detection of PeV-energy gamma rays has placed stringent constraints on the LIV energy scale; in contrast, subluminal LIV can elevate the energy threshold of the $\gamma + \gamma \rightarrow e^+ + e^-$ interaction, enhancing the Universe’s transparency to gamma rays above

10 TeV and potentially enabling the detection of more distant sources. LIV also modifies the threshold energies for interactions like pair production and inverse Compton scattering, altering the development of electromagnetic cascades—such modifications are more pronounced in LIV frameworks. Additionally, LIV-induced changes to cross sections and decay rates, though less explored, may further reshape the gamma-ray flux spectrum at Earth, while the interplay between LIV and background radiation fields (CMB and EBL) influences interaction rates and propagation lengths.

The photon energy in the threshold condition for pair production is modified. This is implemented by replacing ϵ_s with an effective energy (e.g., Finke & Razzaque 2023):

$$\epsilon_s \rightarrow \frac{\epsilon_s}{1 + \frac{1}{4} \left(\frac{\epsilon_s m_e c^2}{E_{QG}} \right)^n \epsilon_s^2}. \quad (16)$$

In this work, we implement the LIV correction solely through this threshold modification (Eq. (16)). Although a complete LIV treatment would also include modifications to the squared interaction amplitude $|M|^2$, the full cross section beyond the simple threshold shift, and potential vacuum processes (e.g., photon decay or vacuum Cherenkov radiation, Carmona et al. (2024)), we focus exclusively on the threshold correction. This choice is motivated by the fact that, in the relevant energy range (TeV-PeV), the threshold shift overwhelmingly dominates the suppression of the optical depth $\tau_{\gamma\gamma}$, while additional amplitude and cross-section changes are subdominant and do not qualitatively alter the transparency enhancement (Carmona et al. 2024; Jacob & Piran 2008). Thus, focusing on the threshold modification captures the leading-order LIV effect on gamma-ray propagation while maintaining computational tractability and model simplicity.

2.4. Joint Effects of ALP-Lorentz Invariance Violation and Model Simplification

Gamma-ray photons originating from TeV sources may undergo continuous interconversion with ALPs as they propagate through various astrophysical environments, including the jet and host galaxy, the intergalactic medium, and the Milky Way. In this process, the potential influence of LIV needs to be considered. When the combined effects of ALPs and LIV are treated in a unified framework, the ALP contribution is fully incorporated through the evolution of the mixing matrix M (Eq. (6)), with the potential LIV effect manifesting itself in this matrix throughout the propagation process.

The LIV contribution, arising from the modified photon dispersion relation in Eq. (15)

under the subluminal case, alters the kinematics of $\gamma\gamma$ pair production. Within a complete effective field theory framework, this modification leads to two primary effects. Firstly, LIV induces a substantial upward shift in the pair-production threshold. To quantify this effect, we evaluate the gamma-ray mean free path λ_γ using an expression for the optical depth $\tau(E, z)$ that explicitly accounts for LIV corrections. The mean free path of a photon with energy E emitted at redshift z is given by (e.g., Long et al. 2020)

$$\lambda_\gamma(E, z) = \frac{D(z)}{\tau(E, z)}, \quad (17)$$

where $D(z)$ denotes the comoving distance to the source. The LIV-induced threshold shift is implemented by replacing the soft-photon energy ϵ_s in Eq. (2) with the effective value defined in Eq. (16) (see, e.g., Carmona et al. 2024). Secondly, LIV introduces an additional energy-dependent correction term,

$$\Delta_{\text{LIV}} \simeq -\frac{1}{2E} \left(\frac{E}{E_{\text{QG}}} \right)^2, \quad (18)$$

which enters directly into the diagonal photon terms Δ_\perp and Δ_\parallel of the mixing matrix M . This correction modifies the photon phase velocities and can further influence the oscillation phases and probabilities of the photon–ALP system during propagation (see, e.g., Galaverni & Sigl 2008).

Gamma-ray photons emitted from a TeV source propagate through the magnetic fields of the jet/host system (S), intergalactic space (I), and the Milky Way (M) before reaching the observer. The general expression for the photon survival probability is:

$$P_{\gamma \rightarrow \gamma} = P_{\gamma \rightarrow \gamma}^{\text{S}} (P_{\gamma \rightarrow \gamma}^{\text{I}} P_{\gamma \rightarrow \gamma}^{\text{M}} + P_{\gamma \rightarrow a}^{\text{I}} P_{a \rightarrow \gamma}^{\text{M}}) + P_{\gamma \rightarrow a}^{\text{S}} (P_{a \rightarrow \gamma}^{\text{I}} P_{\gamma \rightarrow \gamma}^{\text{M}} + P_{a \rightarrow a}^{\text{I}} P_{a \rightarrow \gamma}^{\text{M}}). \quad (19)$$

We neglect photon-ALP mixing in the intergalactic magnetic field (IGMF), such that

$$P_{\gamma \rightarrow \gamma}^{\text{I}} = e^{-\tau_{\gamma\gamma}}, \quad P_{\gamma \rightarrow a}^{\text{I}} = P_{a \rightarrow \gamma}^{\text{I}} = 0. \quad (20)$$

This approximation is justified by the fact that, for typical IGMF strengths $B_{\text{IGMF}} \lesssim 1$ nG and a source redshift $z = 0.151$, the photon-ALP conversion probability remains negligible at the highest energies considered here ($E \gtrsim 10$ TeV). The dominant suppression arises from the weak magnetic field and dephasing effects over cosmological distances, with plasma contributions being subdominant due to the extremely low electron density ($n_e \sim 10^{-7} \text{ cm}^{-3}$

or lower in voids) (Durrer & Neronov 2013; Alves Batista & Saveliev 2021). Although the long propagation path length could partially compensate for the small B_{IGMF} (as encoded in the oscillation probability for large-scale low-B regions, Eq. 21), the net conversion remains negligible in this redshift and energy regime (see, e.g., Long et al. 2021; Chen et al. 2024). We further assume negligible photon-to-ALP conversion in the Milky Way, i.e., $P_{\gamma \rightarrow \gamma}^{\text{M}} \approx 1$, consistent with typical Galactic electron densities and magnetic field geometries along the line of sight to GRB 221009A (see, e.g., Long et al. 2021; Chen et al. 2024). For the source region, we approximate the photon survival probability as $P_{\gamma \rightarrow \gamma}^{\text{S}} \approx 1 - P_{\gamma \rightarrow a}^{\text{S}}$. As discussed in Section 2.3, our treatment of LIV within the ALP framework is intentionally restricted to the modification of the pair-production energy threshold, which enters through the photon mean free path in the propagation matrix M . Within this simplified but well-motivated approach, LIV effects are incorporated solely via the replacement $\tau_{\gamma\gamma} \rightarrow \tau_{\text{LIV},\gamma\gamma}$, as defined in Eq. (16), with all other contributions kept fixed. Under these assumptions, the total photon survival probability simplifies to $P_{\gamma \rightarrow \gamma} \approx (1 - P_{\gamma \rightarrow a}^{\text{S}})e^{-\tau_{\text{LIV},\gamma\gamma}} + P_{\gamma \rightarrow a}^{\text{S}}P_{a \rightarrow \gamma}^{\text{M}}$. Photon-ALP oscillations arise in transverse magnetic fields, with efficiencies set by the competition between the mixing term and other momentum-mismatch contributions. In the strong-mixing regime—realized for sufficiently small (m_a) and/or strong magnetic fields—the conversion becomes efficient and approximately energy independent, the relation $P_{a \rightarrow \gamma} = 2P_{\gamma \rightarrow a}$ holds, as $P_{\gamma \rightarrow a} \rightarrow 1/3$ (see e.g. Long et al. 2020; Chen et al. 2024). In the single domain approximation, the photon conversion probability is given by Mirizzi & Montanino (2009); de Angelis et al. (2011); Galanti & Roncadelli (2018):

$$P_{\gamma \rightarrow a}(E) = \sin^2(2\theta) \sin^2\left(\frac{\Delta_{\text{osc}}L}{2}\right), \quad (21)$$

where

$$\tan(2\theta) = \frac{2\Delta_{a\gamma}}{\Delta_{aa} - \Delta_{\parallel}}, \quad (22)$$

$$\Delta_{\text{osc}} = \sqrt{(\Delta_{aa} - \Delta_{\parallel})^2 + 4\Delta_{a\gamma}^2}. \quad (23)$$

To simplify the modeling of photon-ALP mixing, we neglect the QED vacuum polarization and the CMB-induced photon dispersion terms in the mixing matrix. This is justified by the approximate scaling relations $\Delta_{\text{QED}} \propto E_\gamma \cdot B_T^2$ and $\Delta_{\text{CMB}} \propto E_\gamma \cdot (1+z)^3$. Given that the transverse magnetic field B_T is of the order of a few microgauss and the redshift of the GRB is $z < 0.5$, similar to the case considered in (Chen et al. 2024), both contributions are subdominant compared to the photon-ALP coupling and plasma effects in the energy range of interest.

Additionally, we account for the stochastic orientation of the magnetic field in each

domain, as considered in (Grossman et al. 2002; Chen et al. 2024). When the overall magnetic region has a size $L \gg r$, where r is the coherence length of a single domain and P_0 is the photon-to-ALPs conversion probability within a single domain, the expression for the total conversion probability was originally derived in (Grossman et al. 2002) and is adopted in the present work following the formulation provided by (Chen et al. 2024).

To model the propagation of VHE gamma rays within the source environment, we adopt representative physical parameters for the GRB host galaxy. Specifically, we assume a transverse magnetic field strength of $B_T \simeq 0.5 \mu\text{G}$, an electron density of $n_e \simeq 0.04 \text{ cm}^{-3}$, and a characteristic propagation length of $\sim 10 \text{ kpc}$ (Fletcher 2010). These values are consistent with typical conditions in disk regions of GRB host galaxies and are commonly adopted in similar analyses (e.g., see Chen et al. 2024).

For photon-ALP reconversion in the Milky Way, we follow the Galactic magnetic field model of Jansson & Farrar (2012) and the electron density distribution of Cordes & Lazio (2002), adopting a regular magnetic field strength of $\sim 3.0 \mu\text{G}$, an electron density of $n_e \simeq 0.05 \text{ cm}^{-3}$, and a propagation distance of $\sim 30 \text{ kpc}$ along the line of sight to GRB 221009A (Galactic coordinates $l \simeq 22.4^\circ$, $b \simeq -42.5^\circ$). These parameters are representative of typical Galactic disk conditions. Moreover, the turbulent magnetic field component along this direction is expected to have a limited impact in the strong-mixing regime relevant to our study (Unger & Farrar 2024).

3. Application to GRB 221009A

We utilized the observational data of GRB 221009A from LHAASO (Cao et al. 2023), specifically the measurements from the Kilometer Squared Array (KM2A) and the Water Cherenkov Detector Array (WCDA) during the 300-900 s interval after the trigger. In addition, the Carpet-3 experiment detected gamma-ray photons with energies up to 300 TeV (Dzhappuev et al. 2025). Since the differential flux values at 300 TeV are not explicitly provided in (Dzhappuev et al. 2025), we estimated the upper and lower limits of the 300 TeV flux by assuming time intervals of one hour and one day for temporal differentiation, along with the corresponding average value. This procedure follows the note that the burst duration is poorly constrained, ranging from roughly one hour to an entire day and that the flux can be inferred by dividing the reported differential fluence by the adopted time window.

We perform Bayesian parameter inference using the Python package UltraNest (Buchner 2021) to obtain posterior distributions of model parameters. The LIV-modified EBL optical

depth is calculated using the publicly available `ebtable` package¹ (Meyer 2022), with the EBL model of Finke et al. (2022) adopted throughout this work.

We assess the performance of different photon survival probability models in fitting the observed spectrum of GRB 221009A using the Akaike Information Criterion (AIC), which balances goodness-of-fit against model complexity and penalizes excessive free parameters (see e.g., Akaike 1974). For each scenario, the maximum likelihood \hat{L} is obtained and the AIC is computed as $\text{AIC} = 2k_n - 2\ln(\hat{L})$, where k_n denotes the number of free parameters. The model with the minimum AIC value is identified as the preferred description of the data, providing a quantitative basis for comparing alternative photon survival prescriptions.

We first fit the observed energy spectrum using the ALP-only scenario (Figure 1), obtaining an AIC value of 85.86. For comparison, a fit based solely on the standard EBL model yields a substantially larger AIC of 192.46 and fails to reproduce the emission at both 18 TeV and 300 TeV. Although the ALP-only model successfully accounts for the 18 TeV emission, even the lower envelope of the fitted spectrum falls short of explaining the 300 TeV photon reported by Carpet-3. We then systematically evaluated the photon survival probability within the host galaxy, and Figure 2 demonstrates that for both 18 TeV and 300 TeV photons, at least 70% can escape from the host galaxy into intergalactic space across the explored parameter space of m_a and $g_{a\gamma}$. Given that ALPs alone cannot explain the 300 TeV emission, and that a substantial fraction of very high energy photons can survive the host galaxy, LIV effects may play a crucial role in interpreting the extreme-energy emission of GRB 221009A.

Although LHAASO observations of GRB 221009A set stringent LIV limits ($E_{\text{QG},1} > 10^{20}$ GeV, $E_{\text{QG},2} > 6.9 \times 10^{11}$ GeV at 95% CL) assuming no early time delay (Cao et al. 2024), the Carpet-3 detection of a 300 TeV photon at $T_0 + 4536$ s (Dzhappuev et al. 2025) cannot be explained without new physics, where T_0 is the burst trigger time (Fermi-GBM onset). This photon should be absorbed by the EBL and arrives far too late for standard afterglow models. Ofengeim & Piran (Ofengeim & Piran 2025) demonstrate that only quadratic subluminal LIV simultaneously resolves both the EBL absorption and the late arrival puzzles (Song & Ma 2025), excluding linear ($n = 1$) terms while favoring $\eta_2 = 1.30 \times 10^{-15}$ (95.4% credibility), where η_2 is the dimensionless second-order LIV coefficient. We therefore adopt second-order subluminal LIV with $\eta_2 = 1.30 \times 10^{-15}$ as our physical benchmark.

We also attempted to fit the energy spectrum of GRB 221009A using the previously constrained LIV parameters, without considering the effect of ALPs. As shown in Figure 3, the fitted spectrum for the 300 TeV photon lies slightly below the observed average value

¹<https://github.com/me-manu/ebtable/blob/main/CITATION.cff>

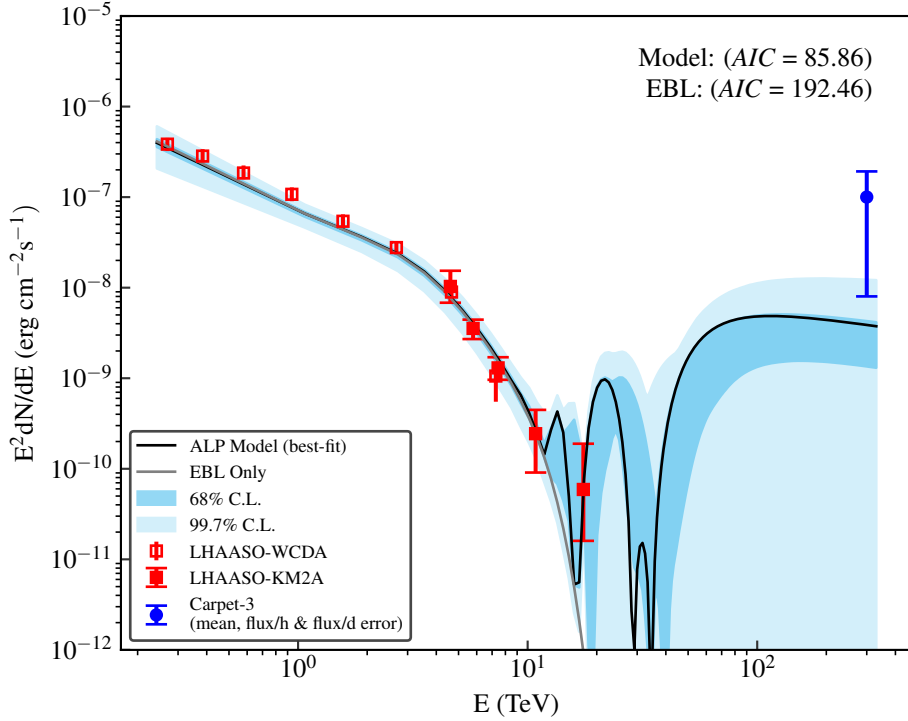


Fig. 1.— Corresponding best-fit SEDs of GRB 221009A under only ALPs scenario with a coupling constant $g_{a\gamma} = 1.489 \times 10^{-10} \text{ GeV}^{-1}$ and $m_a = 4.191 \times 10^{-7} \text{ eV}$. The Carpet-3 point at 300 TeV is derived by dividing the reported differential fluence by time windows of 1 hour (upper bound) and 1 day (lower bound), with the mean shown.

and the value of AIC is 135.33, while the 18 TeV photon cannot be satisfactorily reproduced when accounting only for LIV.

The ALP-only model, while mitigating absorption at 18 TeV, cannot produce sufficient flux at 300 TeV because its oscillatory effect does not sufficiently elevate the pair-production threshold. Conversely, the LIV-only model, which raises this threshold, can allow the 300 TeV photon but tends to overproduce flux in the 10-30 TeV range compared to LHAASO data, as it lacks the energy-dependent modulation introduced by ALP mixing. The hybrid model naturally resolves this: ALP oscillations provide the necessary spectral shaping in the LHAASO band, while the LIV-induced threshold shift is crucial for enabling the survival of the Carpet-3 event.

We next apply the proposed ALP–LIV hybrid model to the TeV-band spectrum of GRB 221009A. For the LIV component, we adopt the quadratic ($n = 2$) energy scale $E_{\text{LIV},2} = 1.30 \times 10^{-7} E_{\text{P1}}$ suggested by Ofengeim & Piran (2025), while the ALP param-

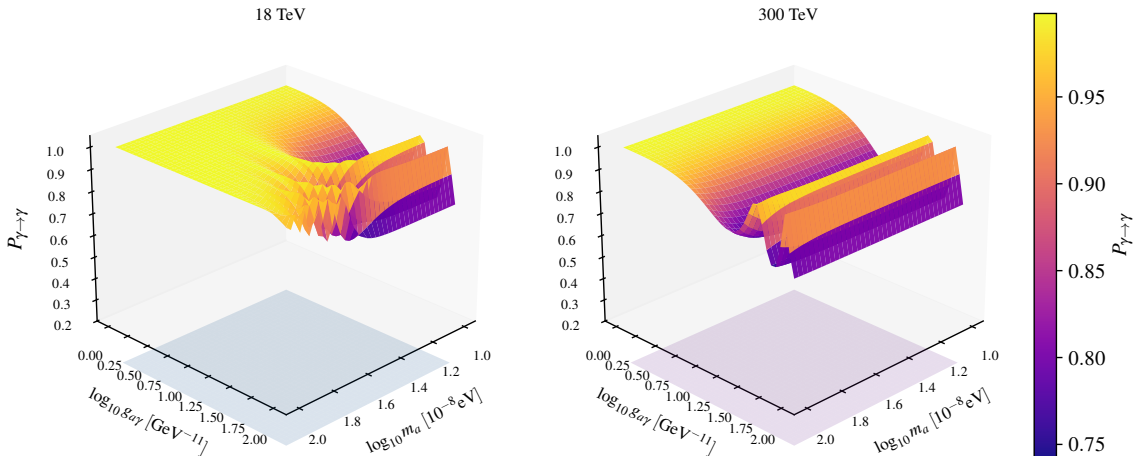


Fig. 2.— Photon survival probability within the host galaxy of GRB 221009A as a function of ALPs mass (m_a) and the ALP-photon coupling constant ($g_{a\gamma}$), evaluated for photon energies of 18 TeV and 300 TeV. The results indicate that a substantial fraction of photons can survive across the explored m_a – $g_{a\gamma}$ parameter space.

eters are treated as free and optimized through spectral fitting. The best-fit values are $g_{a\gamma} = 1.685 \times 10^{-10} \text{ GeV}^{-1}$ and $m_a = 9.545 \times 10^{-8} \text{ eV}$. As illustrated in Figure 4, the hybrid model simultaneously accommodates both the 18 TeV emission and the ~ 300 TeV photon within a unified framework. It yields the lowest Akaike Information Criterion value (AIC = 25.63) among the models considered, indicating a statistically preferred description of the data.

4. Discussion and Conclusions

We have proposed and applied a unified framework that simultaneously incorporates photon–ALP oscillations (via the full evolution of the mixing matrix M , Eq. (6)) and subluminal quadratic LIV effects (manifesting systematically in the average free path and threshold modifications embedded in M). This hybrid ALP-LIV approach provides greater flexi-

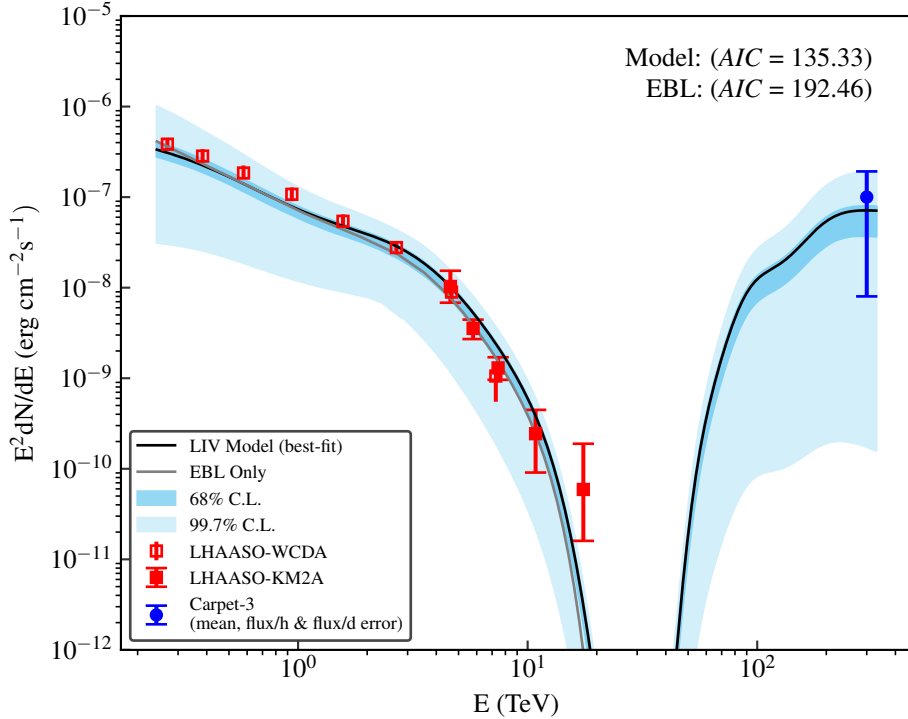


Fig. 3.— Corresponding best-fit SEDs of GRB 221009A under only LIV scenario.

bility and parameter freedom compared to treating either mechanism independently, as the LIV-induced suppression of pair production effectively modulates the effective optical depth over which ALP mixing occurs. We further simplify this unified model and apply the reduced formulation to interpret the multi-band spectral energy distribution of GRB 221009A. The analysis includes LHAASO observations (KM2A and WCDA arrays) during the 300-900 s interval after the trigger, as well as the 300 TeV photon reported by Carpet-3. Since differential flux values at 300 TeV are not explicitly provided in the Carpet-3 report (Dzhappuev et al. 2025), we estimated its upper and lower limits, as well as an average value, by adopting one-hour and one-day time intervals for temporal differentiation. This procedure is consistent with the poorly constrained burst duration, ranging from roughly one hour to one day, and with the method of inferring flux by dividing the reported differential fluence by the chosen time window.

It is important that, in our model, LIV scenarios will introduce a preferred reference frame, commonly identified with the CMB comoving frame, photon-ALP mixing is naturally formulated in the local frame defined by the magnetic field. The relative velocity between these frames is of order ($v_{\text{pec}} \sim 10^{-3}c$), as inferred from the CMB dipole. Corrections induced

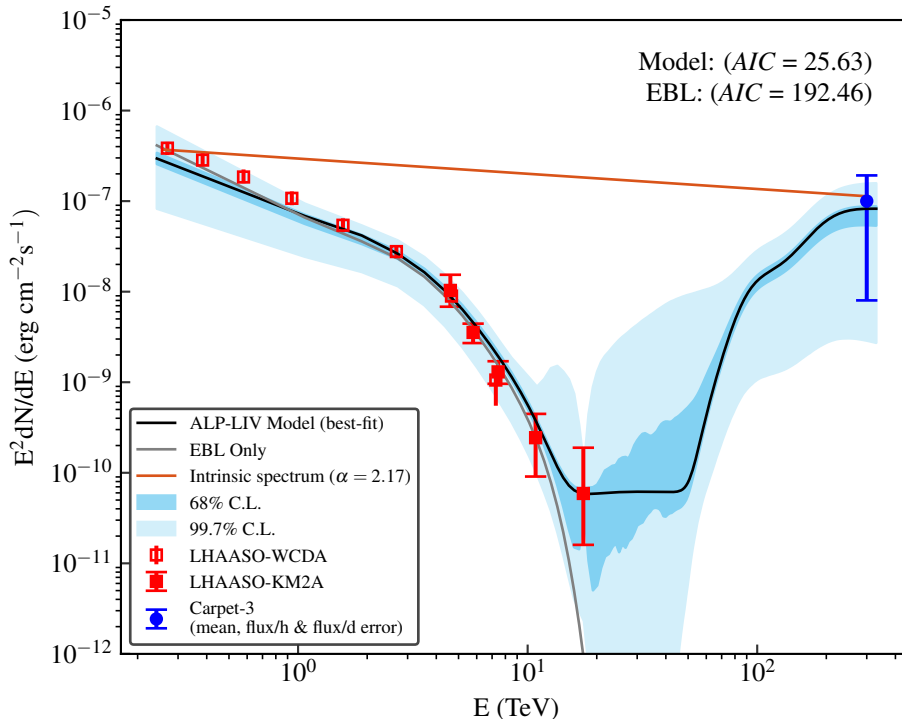


Fig. 4.— Corresponding best-fit SEDs of GRB 221009A under ALP-LIV hybrid scenario with a coupling constant $g_{a\gamma} = 1.685 \times 10^{-10} \text{ GeV}^{-1}$, $m_a = 9.545 \times 10^{-8} \text{ eV}$.

by boosting LIV-modified dispersion relations to the local frame are therefore suppressed by this small factor and remain subdominant with respect to the already highly suppressed LIV terms themselves. Consequently, the use of a common local propagation frame does not affect our results (e.g., Mattingly 2005). Besides, We only account for LIV effects exclusively via the $\gamma\gamma$ pair-production threshold modification. Although a complete LIV treatment would include changes to interaction amplitudes, cross sections, and additional vacuum processes, these effects are subdominant in the TeV–PeV regime. The threshold shift dominates the suppression of optical depth ($\tau_{\gamma\gamma}$) and therefore captures the leading LIV contribution to gamma-ray transparency.

More generally, several deliberate simplifications are adopted in this work to construct a tractable and physically transparent first-order framework. In particular, photon-ALP mixing in the IGMF is neglected. This approximation is well justified for weak intergalactic fields ($B_{\text{IGMF}} \lesssim 1 \text{ nG}$) and for the redshift of GRB 221009A, where plasma effects dominate at the highest energies considered and suppress efficient photon–ALP conversion. We note, however, that in scenarios involving stronger or more structured IGMFs, additional

conversion could occur, potentially shifting the preferred ALP parameter space.

Likewise, we deliberately adopt only the EBL model of Finke et al. (2022). This model represents one of the most up-to-date EBL frameworks and is tightly constrained by a broad range of observational inputs, including luminosity densities, stellar mass functions, dust attenuation, and γ -ray absorption measurements, making it particularly well suited for the energy range ($\gtrsim 10$ TeV) explored here. Comparisons with other widely used EBL models (e.g., Saldana-Lopez et al. 2021; Gilmore et al. 2012) indicate that differences in the predicted optical depths above 10 TeV are typically within $\sim 30\%$, well below the dominant systematic uncertainties associated with current VHE observations. Consequently, restricting our analysis to a single, well-motivated EBL model does not compromise the robustness of our main conclusions.

We further adopt representative average parameters for the magnetic fields and electron densities in both the GRB host galaxy and the Milky Way, following standard practice in the literature. While line-of-sight variations and environmental inhomogeneities could affect the precise photon-ALP conversion probabilities, they are unlikely to qualitatively alter the key conclusion that a high photon survival fraction is achievable. For LIV, we focus on the dominant modification of the pair-production threshold, which captures the leading effect relevant for enhanced transparency at ultra-high energies. A more complete effective-field-theory treatment could introduce subdominant spectral corrections, but these are not expected to overturn our main results. Taken together, these modeling choices demonstrate that the success of the ALP-LIV hybrid scenario does not stem from over-parameterization, but rather from its underlying physical mechanisms.

Finally, we note that VHE gamma rays propagating through the Milky Way may experience additional attenuation via electron-positron pair production on the interstellar radiation field (ISRF), whose optical depth depends sensitively on the line of sight (Porter et al. 2017; Di Marco et al. 2025). For GRB 221009A, which is located at relatively high Galactic latitude, ISRF-induced absorption is expected to be weak and does not qualitatively affect our conclusions within the simplified framework adopted here. Future studies could incorporate line-of-sight-dependent Galactic models, such as detailed electron density and radiation-field distributions (e.g., Yao et al. 2017), to further assess the impact of these environmental uncertainties on photon survival probabilities.

The explored ALP parameter space spans $\log_{10}(m_a/10^{-8} \text{ eV}) \in [-2, 1]$ and $\log_{10}(g_{a\gamma}/\text{GeV}^{-1}) \in [-12, -9]$, consistent with current experimental and astrophysical bounds. For the LIV component, we fix the quadratic ($n = 2$) coefficient to $\eta_2 = 1.30 \times 10^{-15}$, corresponding to an energy scale $E_{\text{LIV},2} = 1.30 \times 10^{-7} E_{\text{P1}}$, as suggested by recent analyses of the Carpet-3 ~ 300 TeV photon (Ofengeim & Piran 2025). That study favors a quadratic subluminal mod-

ification at the 95.4% credibility level while disfavoring linear ($n = 1$) LIV contributions. Independent constraints derived solely from LHAASO observations of GRB 221009A yield limits of $E_{\text{QG},2} \gtrsim (6\text{--}10) \times 10^{11}$ GeV (Cao et al. 2024), corresponding to $|\eta_2| \lesssim 10^{-14} - 10^{-15}$ depending on the specific formulation. Our adopted value therefore lies comfortably within, or close to, the allowed parameter space. Tighter exclusions reported from other GRBs or blazar observations mainly constrain linear or superluminal LIV scenarios, leaving quadratic subluminal effects at this level viable. For the ALP component, the coupling $g_{a\gamma}$ and mass m_a are treated as free parameters and optimized through spectral fitting. As shown in Figure 2, across the explored m_a - $g_{a\gamma}$ parameter space, at least $\sim 70\%$ of the 18 TeV and 300 TeV photons are able to escape the host galaxy. This high survival fraction implies that LIV-induced modifications remain significant even with efficient photon-ALP conversion.

As shown in Figures 1, 3, and 4, the hybrid ALP–LIV model successfully reproduces both the 18 TeV emission detected by LHAASO and the ~ 300 TeV photon reported by Carpet-3, yielding the lowest AIC value of 25.63 among all considered models. In the ALP-only scenario, the best-fit parameters are $g_{a\gamma} = 1.489 \times 10^{-10}$, GeV^{-1} and $m_a = 4.191 \times 10^{-7}$, eV; however, this model fails to reproduce even the lower bound of the observed 300 TeV flux, resulting in a significantly larger AIC of 85.86. Conversely, the LIV-only scenario with quadratic ($n = 2$) dispersion modifications slightly underestimates the 300 TeV flux and cannot adequately account for the 18 TeV emission, yielding an AIC of 135.33. Only the combined ALP–LIV framework, with best-fit parameters $g_{a\gamma} = 1.685 \times 10^{-10}$, GeV^{-1} and $m_a = 9.545 \times 10^{-8}$, eV, provides an excellent and self-consistent description of all available observational data. In addition, we also performed spectral fitting to the multi-wavelength data of GRB 221009A using a standard EBL absorption model alone. As shown in Fig. 1,3,4, the resulting spectrum fails to account for the emission at both 18 TeV and ~ 300 TeV, and yields a substantially larger Akaike information criterion value, $\text{AIC}=192.46$, indicating a poor description of the data.

A key issue is whether the inferred parameters are compatible with independent constraints from other experiments and observations. For the ALP sector, a coupling $g_{a\gamma} \sim 10^{-10}$, GeV^{-1} at $m_a \sim 10^{-7}$, eV lies close to the upper envelope of current limits but is not formally excluded. Searches for spectral irregularities in blazar samples with *Fermi*-LAT (e.g., Ajello et al. 2016), as well as stacked analyses of Galactic and extragalactic sources, typically constrain $g_{a\gamma} \gtrsim (0.5\text{--}1) \times 10^{-10}$, GeV^{-1} in the neV– μeV mass range at 95% confidence, with complementary bounds from helioscope experiments such as CAST at lower masses. These limits generally assume dominant ALP–photon mixing in Galactic or intergalactic magnetic fields and rely on null detections of oscillatory features. In contrast, our scenario exploits specific line-of-sight magnetic-field configurations together with an additional LIV-induced enhancement of transparency, which can partially relax constraints

derived under pure-ALP assumptions. As a result, no direct inconsistency arises: the favored parameters are marginally compatible with existing bounds or reside in comparatively less constrained regions once the LIV contribution is included.

In our fits, the ALP parameters primarily affect the spectral shape in the 10–30 TeV range, while LIV dominates above 100 TeV. Concerning possible degeneracies between ALP and LIV parameters, we find that the two mechanisms are not strongly degenerate within the parameter space explored here. ALP-photon mixing, which is oscillatory and magnetic-field dependent, primarily affects photon survival through conversion and reconversion processes, whereas LIV acts by systematically modifying the $\gamma\gamma$ pair-production threshold and, consequently, the effective propagation encoded in the mixing matrix M . These effects are therefore complementary. ALPs can induce spectral hardening or modulations over specific energy ranges, while quadratic subluminal LIV produces a monotonic increase in transparency at the highest energies ($E \gtrsim 10\text{--}100$ TeV), enabling a natural explanation of the Carpet-3 ~ 300 TeV event without overproducing the LHAASO flux at lower energies. Fits to the combined LHAASO and Carpet-3 spectrum confirm that ALP-only models struggle to accommodate the ultra-high-energy data, LIV-only models yield only modest improvements in the TeV regime, and the hybrid ALP-LIV scenario provides a significantly improved description across the full 10–300 TeV range.

We note, however, that degeneracies could emerge in other regions of parameter space. For example, stronger ALP couplings combined with weaker LIV effects (or vice versa) might reproduce similar photon survival probabilities at specific energies or redshifts. Such degeneracies are more likely for smaller $g_{a\gamma}$ or larger m_a , where ALP effects diminish, or for alternative LIV orders and energy scales. A comprehensive exploration of the joint $(g_{a\gamma}, m_a, \eta_2)$ parameter space would be required to fully quantify these possibilities, ideally informed by future observations with CTA, or next-generation GRB detections. Within the parameter region favored by GRB 221009A, however, we find no evidence for strong degeneracy, supporting the interpretation that the observed extreme-energy transparency arises from a genuine synergistic interplay between ALP mixing and LIV effects.

This work develops a unified hybrid framework that combines ALP oscillations with LIV to account for the anomalous transparency of the Universe to ultra-high-energy gamma rays from GRB 221009A. In contrast to previous studies that typically considered ALP and LIV effects separately, such as Galanti & Roncadelli (2025), who focused primarily on pure LIV-induced threshold modifications and associated time delays, however, we perform a joint Bayesian analysis of the time-resolved TeV spectrum, incorporating both the LHAASO data in the 300–900 s interval and the ~ 300 TeV Carpet-3 event. Our results quantitatively show that neither ALP nor LIV alone can simultaneously reproduce the observed 18 TeV and

300 TeV photons, whereas their combination provides a statistically preferred description of the data, as quantified by the AIC.

In addition, our results are broadly consistent with those of Satunin & Troitsky (2025), who also investigated an ALP+LIV scenario for GRB 221009A and found that a joint mechanism is required to explain the observed spectrum. Key differences lie in our use of time-resolved differential fluxes rather than integrated fluence, a more careful treatment of the flux uncertainty associated with the 300 TeV photon through both one-hour and one-day temporal windows, and the adoption of the quadratic subluminal LIV benchmark motivated by Ofengeim & Piran (2025). These methodological choices allow for a more detailed characterization of the afterglow-phase emission and the sensitivity of the inferred parameters. While some aspects of the ALP–LIV implementation in Satunin & Troitsky (2025) are formulated differently, their analysis provides valuable complementary support for the viability of the hybrid scenario. Finally, we emphasize that our work is not intended to be a fine-tuned solution tailored solely to the high-energy spectrum of GRB 221009A. Rather, we aim to construct a self-consistent and physically motivated ALP-LIV hybrid framework, which can be applied more generally to make testable predictions for the propagation and detection of gamma-ray photons with energies $\gtrsim 10$ TeV in future observations.

Taken together, our analysis demonstrates that the anomalous transparency of GRB 221009A at energies extending from ~ 10 TeV up to the ~ 300 TeV regime cannot be accommodated by standard EBL absorption, nor by ALP or LIV effects acting in isolation. Instead, a hybrid ALP–LIV framework provides a unified and physically consistent explanation, in which photon-ALP oscillations and quadratic subluminal LIV act in complementary ways to enhance photon survival over cosmological distances. In this framework, the observed 18 TeV and ~ 300 TeV events are simultaneously reproduced with the best overall statistical performance among the tested scenarios, while standard EBL-only, ALP-only, or LIV-only models fail to do so. By adopting literature-motivated LIV parameters and simplified but well-justified astrophysical environments, we show that this agreement arises from the core physical mechanisms of the model rather than from excessive freedom in parameter choice, establishing the ALP-LIV synergy as a viable interpretation of the GRB 221009A observations.

Looking ahead, the enhanced sensitivity of the Cherenkov Telescope Array (CTA) will be crucial for detecting a larger sample of > 10 TeV photons from GRBs and AGN, enabling detailed spectral studies capable of distinguishing oscillatory transparency features characteristic of ALP-induced effects from the monotonic behavior expected in LIV scenarios. Independent constraints on LIV from future GRB time-delay analyses (e.g., Cao et al. 2024), together with dedicated ALP searches by next-generation experiments such as

the International Axion Observatory (IAXO; Irastorza et al. (2011)), will probe the ALP coupling–mass parameter space down to $g_{a\gamma} \sim 10^{-12}\text{--}10^{-10} \text{ GeV}^{-1}$ for $m_a \sim 10^{-3}\text{--}10^{-2} \text{ eV}$. This region partially overlaps with, yet remains complementary to, the higher-mass and lower-coupling parameter space explored by very-high-energy gamma-ray spectral modeling, including the present work. Such complementarity will enable progressively more stringent tests of the hybrid ALP–LIV framework. In parallel, implementing LIV-modified absorption self-consistently within public gamma-ray propagation frameworks (e.g., through extensions of **gammaALPs**; Meyer et al. (2022)) will allow this hybrid scenario to be applied to source populations, enabling robust statistical tests. More comprehensive implementations within advanced propagation codes such as **CRPropa**, incorporating existing modules for LIV (Saveliev & Alves Batista 2024) and ALP effects (Alves Batista et al. 2023), would further enable detailed Monte Carlo simulations of electromagnetic cascades and population-level studies. The detection of GRB 221009A thus highlights a possible interplay between particle physics beyond the Standard Model and quantum-gravity effects. Our hybrid ALP–LIV framework provides a concrete, testable paradigm for this synergy, making specific predictions for the very-high-energy sky that forthcoming observatories will be well positioned to probe.

The authors would like to thank the anonymous referee for the helpful comments, which improved the manuscript significantly. The authors gratefully acknowledge the financial supports from the National Natural Science Foundation of China (grants 12063005, 12063006, 12233006, U2031111), the program for Innovative Research Team (in Science and Technology) in University of Yunnan Province (IRTSTYN), the program for Reserve Talents of Young, Middle-aged Academic and Technical Leaders in Yunnan Province (grant 202205AC160087, 202405AC350114), the program for Hunan Outstanding Youth Science Foundation (2024JJ2040) and the Special Basic Cooperative Research Programs of Yunnan Provincial Undergraduate Universities’ Association (grants NO.202501BA070001-122). The authors gratefully acknowledge the computing support provided by the JRT Science Data Center at Yuxi Normal University and Q.L.H. gratefully acknowledges the kind and selfless help from Prof. Nikita Pozdnukhov (Dzhappuev et al. 2025) and Prof. Domínguez, A.(Domínguez et al. 2013).

REFERENCES

- Abbott, L. F. & Sikivie, P. 1983, *Physics Letters B*, 120, 1-3, 133. doi:10.1016/0370-2693(83)90638-X

- Abdo, A. A., Ackermann, M., Ajello, M., et al. 2009, *Nature*, 462, 7271, 331.
doi:10.1038/nature08574
- Acciari, V. A., Ansoldi, S., Antonelli, L. A., et al. 2020, *Phys. Rev. Lett.*, 125, 2, 021301.
doi:10.1103/PhysRevLett.125.021301
- Aharonian, F., Akhperjanian, A. G., Bazer-Bachi, A. R., et al. 2006, *Nature*, 440, 7087, 1018. doi:10.1038/nature04680
- Ajello, M., Albert, A., Anderson, B., et al. 2016, *Phys. Rev. Lett.*, 116, 16, 161101.
doi:10.1103/PhysRevLett.116.161101
- Akaike, H. 1974, *IEEE Transactions on Automatic Control*, 19, 716.
doi:10.1109/TAC.1974.1100705
- Alves Batista, R. & Saveliev, A. 2021, *Universe*, 7, 7, 223. doi:10.3390/universe7070223
- Alves Batista, R., Viviente, C., Di Marco, G., et al. 2023, arXiv:2308.00935.
doi:10.48550/arXiv.2308.00935
- Amelino-Camelia, G., Ellis, J., Mavromatos, N. E., et al. 1998, *Nature*, 393, 6687, 763.
doi:10.1038/31647
- Bassan, N., Mirizzi, A., & Roncadelli, M. 2010, *J. Cosmology Astropart. Phys.*, 2010, 5, 010.
doi:10.1088/1475-7516/2010/05/010
- Biteau, J. & Williams, D. A. 2015, *ApJ*, 812, 60. doi:10.1088/0004-637X/812/1/60
- Buchner, J. 2021, *The Journal of Open Source Software*, 6, 3001. doi:10.21105/joss.03001
- Cao, Z., Chen, M.-J., Chen, S.-Z. H., et al. 2019, *Chinese Astron. Astrophys.*, 43, 457.
doi:10.1016/j.chinastron.2019.11.001
- Cao, Z., Aharonian, F., An, Q., et al. 2023, *Science Advances*, 9, eadj2778.
doi:10.1126/sciadv.adj2778
- Cao, Z., Aharonian, F., Axikegu, B., et al. 2024, *Phys. Rev. Lett.*, 133, 7, 071501.
doi:10.1103/PhysRevLett.133.071501
- Carmona, J. M., Cortés, J. L., Rescic, F., et al. 2024, *Phys. Rev. D*, 110, 6, 063035.
doi:10.1103/PhysRevD.110.063035
- Chen, Y.-C., Chen, S., Huang, W.-C., et al. 2024, , arXiv:2411.08577.
doi:10.48550/arXiv.2411.08577

- Conlon, J. P. 2006, *Journal of High Energy Physics*, 2006, 5, 078. doi:10.1088/1126-6708/2006/05/078
- Cordes, J. M. & Lazio, T. J. W. 2002, , *astro-ph/0207156*. doi:10.48550/arXiv.astro-ph/0207156
- de Angelis, A., Mansutti, O., & Roncadelli, M. 2008, *Physics Letters B*, 659, 5, 847. doi:10.1016/j.physletb.2007.12.012
- de Angelis, A., Galanti, G., & Roncadelli, M. 2011, *Phys. Rev. D*, 84, 10, 105030. doi:10.1103/PhysRevD.84.105030
- De Angelis, A., Galanti, G., & Roncadelli, M. 2013, *MNRAS*, 432, 4, 3245. doi:10.1093/mnras/stt684
- de Ugarte Postigo, A., Izzo, L., Pugliese, G., et al. 2022, *GRB Coordinates Network, Circular Service*, No. 32648, 32648
- Di Marco, G., Alves Batista, R., & Sánchez-Conde, M. A. 2025, *Phys. Rev. D*, 111, 8, 083004. doi:10.1103/PhysRevD.111.083004
- Dobrynina, A., Kartavtsev, A., & Raffelt, G. 2015, *Phys. Rev. D*, 91, 8, 083003. doi:10.1103/PhysRevD.91.083003
- Domínguez, A., Finke, J. D., Prada, F., et al. 2013, *ApJ*, 770, 77. doi:10.1088/0004-637X/770/1/77
- Durrer, R. & Neronov, A. 2013, *A&A Rev.*, 21, 62. doi:10.1007/s00159-013-0062-7
- Dzhappuev, D. D., Afashokov, Y. Z., Dzaparova, I. M., et al. 2022, *The Astronomer’s Telegram*, 15669, 1.
- Dzhappuev, D. D., Dzaparova, I. M., Dzhatdov, T. A., et al. 2025, *Phys. Rev. D*, 111, 10, 102005. doi:10.1103/PhysRevD.111.102005
- Ellis, J., Mavromatos, N. E., & Nanopoulos, D. V. 2008, *Physics Letters B*, 665, 5, 412. doi:10.1016/j.physletb.2008.06.029
- Ellis, J., Konoplich, R., Mavromatos, N. E., et al. 2019, *Phys. Rev. D*, 99, 8, 083009. doi:10.1103/PhysRevD.99.083009
- Finke, J. D., Ajello, M., Domínguez, A., et al. 2022, *ApJ*, 941, 1, 33. doi:10.3847/1538-4357/ac9843

- Finke, J. D. & Razzaque, S. 2023, *ApJ*, 942, L21. doi:10.3847/2041-8213/acade1
- Fletcher, A. 2010, *The Dynamic Interstellar Medium: A Celebration of the Canadian Galactic Plane Survey*, 438, 197. doi:10.48550/arXiv.1104.2427
- Galaverni, M. & Sigl, G. 2008, *Phys. Rev. Lett.*, 100, 2, 021102. doi:10.1103/PhysRevLett.100.021102
- Galanti, G. & Roncadelli, M. 2018, *Phys. Rev. D*, 98, 4, 043018. doi:10.1103/PhysRevD.98.043018
- Galanti, G. & Roncadelli, M. 2025, , arXiv:2504.01830. doi:10.48550/arXiv.2504.01830
- Gilmore, R. C., Somerville, R. S., Primack, J. R., et al. 2012, *MNRAS*, 422, 3189. doi:10.1111/j.1365-2966.2012.20841.x
- Gould, R. J. & Schröder, G. P. 1967, *Physical Review*, 155, 5, 1404. doi:10.1103/PhysRev.155.1404
- Grossman, Y., Roy, S., & Zupan, J. 2002, *Physics Letters B*, 543, 23. doi:10.1016/S0370-2693(02)02448-6
- Horns, D., Maccione, L., Meyer, M., et al. 2012, *Phys. Rev. D*, 86, 7, 075024. doi:10.1103/PhysRevD.86.075024
- Irastorza, I. G., Avignone, F. T., Caspi, S., et al. 2011, *J. Cosmology Astropart. Phys.*, 2011, 6, 013. doi:10.1088/1475-7516/2011/06/013
- Jacob, U. & Piran, T. 2008, *Phys. Rev. D*, 78, 12, 124010. doi:10.1103/PhysRevD.78.124010
- Jansson, R. & Farrar, G. R. 2012, *ApJ*, 757, 1, 14. doi:10.1088/0004-637X/757/1/14
- Kifune, T. 1999, *ApJ*, 518, 1, L21. doi:10.1086/312057
- Lehnert, R. & Potting, R. 2004, *Phys. Rev. Lett.*, 93, 11, 110402. doi:10.1103/PhysRevLett.93.110402
- Long, G. B., Lin, W. P., Tam, P. H. T., et al. 2020, *Phys. Rev. D*, 101, 6, 063004. doi:10.1103/PhysRevD.101.063004
- Long, G., Chen, S., Xu, S., et al. 2021, *Phys. Rev. D*, 104, 8, 083014. doi:10.1103/PhysRevD.104.083014
- MAGIC Collaboration, Albert, J., Aliu, E., et al. 2008, *Science*, 320, 5884, 1752. doi:10.1126/science.1157087

- Mattingly, D. 2005, *Living Reviews in Relativity*, 8, 1, 5. doi:10.12942/lrr-2005-5
- Meyer, M. 2022, Zenodo, v0.5. doi:10.5281/zenodo.7312062
- Meyer, M., Davies, J., & Kuhlmann, J. 2022, 37th International Cosmic Ray Conference, 557. doi:10.22323/1.395.0557
- Mirizzi, A. & Montanino, D. 2009, *J. Cosmology Astropart. Phys.*, 2009, 12, 004. doi:10.1088/1475-7516/2009/12/004
- Ofengeim, D. D. & Piran, T. 2025, *Phys. Rev. D*, 112, 8, 083055. doi:10.1103/cydc-6j4z
- Peccei, R. D. & Quinn, H. R. 1977, *Phys. Rev. Lett.*, 38, 25, 1440. doi:10.1103/PhysRevLett.38.1440
- Porter, T. A., Jóhannesson, G., & Moskalenko, I. V. 2017, *ApJ*, 846, 1, 67. doi:10.3847/1538-4357/aa844d
- Qin, L., Wang, J., Gao, Q., et al. 2023, *MNRAS*, 521, 6219. doi:10.1093/mnras/stad531
- Raffelt, G. & Stodolsky, L. 1988, *Phys. Rev. D*, 37, 5, 1237. doi:10.1103/PhysRevD.37.1237
- Saldana-Lopez, A., Domínguez, A., Pérez-González, P. G., et al. 2021, *MNRAS*, 507, 5144. doi:10.1093/mnras/stab2393
- Satunin, P. S. & Troitsky, S. V. 2025, , arXiv:2510.07234. doi:10.48550/arXiv.2510.07234
- Saveliev, A. & Alves Batista, R. 2024, *Classical and Quantum Gravity*, 41, 11, 115011. doi:10.1088/1361-6382/ad40f1
- Stecker, F. W. & Glashow, S. L. 2001, *Astroparticle Physics*, 16, 1, 97. doi:10.1016/S0927-6505(01)00137-2
- Song, H. & Ma, B.-Q. 2025, *Physics Letters B*, 870, 139959. doi:10.1016/j.physletb.2025.139959
- Unger, M. & Farrar, G. R. 2024, *ApJ*, 970, 1, 95. doi:10.3847/1538-4357/ad4a54
- Yao, J. M., Manchester, R. N., & Wang, N. 2017, *ApJ*, 835, 1, 29. doi:10.3847/1538-4357/835/1/29
- Zheng, Y. G., Kang, S. J., Zhu, K. R., et al. 2023, *Phys. Rev. D*, 107, 8, 083001. doi:10.1103/PhysRevD.107.083001